Journal of
Polymer & Composites

ISSN: 2321-2810 (Online)
ISSN: 2321-8525 (Print)
Volume 14, Special Issue 2, 2026
DOI (Journal): 10.37591/JoPC

STM JOURNALS

https://journals.stmjournals.com/jopc

Research JoPC

AI-Accelerated Development of Gradient Polymer Nanocomposite Thin Films

M. Nithin Srinivas[1,*], S.N. Padhi[2]

Abstract

Gradient polymer nanocomposite thin films are an active field of materials research due to the fact that it enables scientists to de-facto regulate the optical, electrical, and mechanical properties of a film by merely altering its composition on a layer-by-layer basis. This type of control opens the gate to the improved flexible electronics, long lasting protective coats, and the new smart gadgets. The problem is, though, that it is a tedious process of trial and error to develop these gradients. It can be that researchers need to test dozens of experimental combinations before discovering the appropriate mixture of materials. This paper presents an AI-based solution that will help speed up that process significantly. We combine high-throughput film fabrication, machine learning models, and automated optimization tools in our framework to assist with the task of designing gradient nanocomposite films in a fraction of the standard time. We constructed a database of 420 movies where the concentrations of silver nanoparticles and graphene oxide are at various proportions, with a thickness range of 100150 to 500 nanometers thick. Based on this information, convolutional neural networks were trained to examine microscopy images and property measurements, with 94 percent accuracy depending on the prediction of the performance of a film. Then we combined genetic algorithms with surrogate models so that we could rapidly find the optimal pattern of gradients. This optimization step identified promising designs in only 48 hours 95 percent time savings versus the normal research techniques. The optimized films recorded remarkable progress when subjected to experimentation that was characterized by an increase in conductivity, transparency as well as much greater flexibility. In general, this machine-assisted AI-based approach transforms the principles of developing thin films to be less of a guesswork and more of a forecast-based design.

Keywords: Gradient thin film, polymer nanocomposites, artificial intelligence, machine learning, high-throughput synthesis, flexible electronics.

INTRODUCTION

Polymer films with nanoparticles have become important materials in the next-generation electronics, sensors and energy devices [1]. These nanocomposites can combine the functionalities that are impossible with either component on its own as they combine the ease with which polymers can be processed and the superior properties of nanomaterials [2]. Recent developments have demonstrated that by addition of composition gradients, systematic spatial difference in nanoparticle concentration, performance can be radically improved through property gradient optimization of multiple functions at once [3].

The idea is inspired by the natural materials such as bone and bamboo, which have graded structures which spread the stress effectively and catastrophic failure is avoided [4]. Gradients in thin films

***Author for Correspondence**
M. Nithin Srinivas

[1]M. Tech Student, Department of Mechanical Engineering, Koneru Laksmaiah Education Foundation, Vaddeswaram, Guntur District, Andhra Pradesh, India
[2]Professor, Department of Mechanical Engineering, Koneru Laksmaiah Education Foundation, Vaddeswaram, Guntur District, Andhra Pradesh, India

Received Date: December 29, 2025
Accepted Date: February 05, 2026
Published Date: April 08, 2026

Citation: M. Nithin Srinivas, S.N. Padhi. AI-Accelerated Development of Gradient Polymer Nanocomposite Thin Films. Journal of Polymer & Composites. 2026; 14 (Special Issue 2): S456–S469p.

facilitate a gradual change between layers when their properties vary, eliminating interfacial stresses, improving their adhesion and permitting the surface and bulk properties to be independently optimized [5]. As an illustration, a conductive transparent film could most effectively achieve the highest concentration of nanoparticles on a single side of the surface to be conductive, and still remain transparent by being depleted gradually on the other side [6].

Gradient nanocomposite film development is not easy, although it has been promised. Design space is huge - composition profiles are capable of following linear, exponential, sigmoidal or custom functions, with nanoparticle concentrations across nanometer-scale thicknesses [7]. Classical development is based on trial and error: create candidate films, describe properties, change parameters and cycle. This is a process that normally takes months or years and is investigative of a minute percent of potential designs [8].

Artificial intelligence is a paradigm shift. Machine learning algorithms are capable of learning highly complicated process-condition-composition-property relationships based on experimental data [9]. These models are able to predict the performance of unexplored designs in milliseconds once trained so that they can quickly be screened virtually [10]. In combination with automatic optimization algorithms, AI has the potential to search large design spaces in a systematic manner to find the best solution [11]. The last achievements in the field of drug discovery, the design of materials, and optimization of the process show how AI can be transformative [12].

This paper introduces a hybrid AI-accelerated architecture of making gradient polymer nanocomposites thin films. The scheme is shown with respect to transparent conductive films that contain silver nanoparticles and graphene oxide within polyvinyl alcohol producing materials, but the strategy extends to a wide range of materials and applications.

MATERIALS AND METHODS

Material System

The choice of polyvinyl alcohol (PVA) was based on the fact that the polymer is an ideal film-forming material, transparent, and aqueous processable [13]. Silver nanoparticles (AgNPs, 20-40 nm diameter) have been used to provide electrical conductivity whereas graphene oxide (GO, 1-5 µm lateral size, 1-2 nm thickness) has been used to augment mechanical properties and thermal stability [14]. Commercial vendors provided all of the materials, which were not purified. High-throughput film synthesis involves growing multiple films simultaneously, typically on a substrate, through the enhancement of chimeric chemisensing (chemistotransduction).

High-Throughput Film Synthesis

High-throughput film synthesis is the growth of many films at a time, usually on a substrate, by increasing chimeric chemisensing (chemistotransduction). Movies were produced by another automated layer by layer spin coating system invented in-house. The system has the ability to control: - Solution composition (0-5 wt% AgNP, 0-3 wt% GO) - Spin speed (1000-5000 rpm) - Layer thickness (10-50 nm per layer) - Drying conditions (temperature, humidity, time) in particular.

Gradient films Gradient films were prepared by laying on 5-20 sequential layers with programmatically different concentrations of nanoparticles. Film total thickness was between 100-500 nm. It was a self-sustaining system that produced 12-15 films daily and had limited man working on it.

Characterization Suite

Both movies were thoroughly characterized

- *Optical Properties:* UV-Vis spectroscopy: Transmittance 550 nm - Spectral analysis: 300-800 nm range
- *Electrical Properties:* Four-point probe: Sheet resistance (Omega/Squares)- Conductivity calculation: sigma=1/Rs t.

- *Mechanical Profile:* Nanoindentation: Elastic moduli, hardness - Bending tests Flexibility, crack resistance
- *Microstructural Analysis:* Cross-sectional SEM: Gradient profile check - AFM: Surface roughness - XRD: Nanoparticle dispersion.

Dataset Generation

We made 420 systematically varied sort of gradient films with nanoparticles: AgNP (0-5 wt%) at varying concentrations, GO (0-3 wt%) at varying concentrations, with - layer counts (5-20 layers) and - thickness (100-500 nm) of the films. The 85 features used to represent each film were: - Layer-wise compositions - Gradient function parameters - Processing conditions - Measured microstructural characteristics. Target properties were transmittance, conductivity, elastic modulus and index of flexibility. The architecture of machine learning is presented and explained in this section.

Machine Learning Architecture

Convolutional Neural Network (CNN) Microstructure

Our CNN to cross-sectional SEM image gradient profiles was designed to predict. The architecture was: -Input: 512512 pixel grayscale images - 5 convolutional layers (32, 64, 128, 256, 512 filters) - Max pooling and dropout to regularize the architecture - 2 fully connected layers (256, 128 neurons) - Output: Concentration profile (20 values) The CNN was 94% accurate at reconstructing the profile.

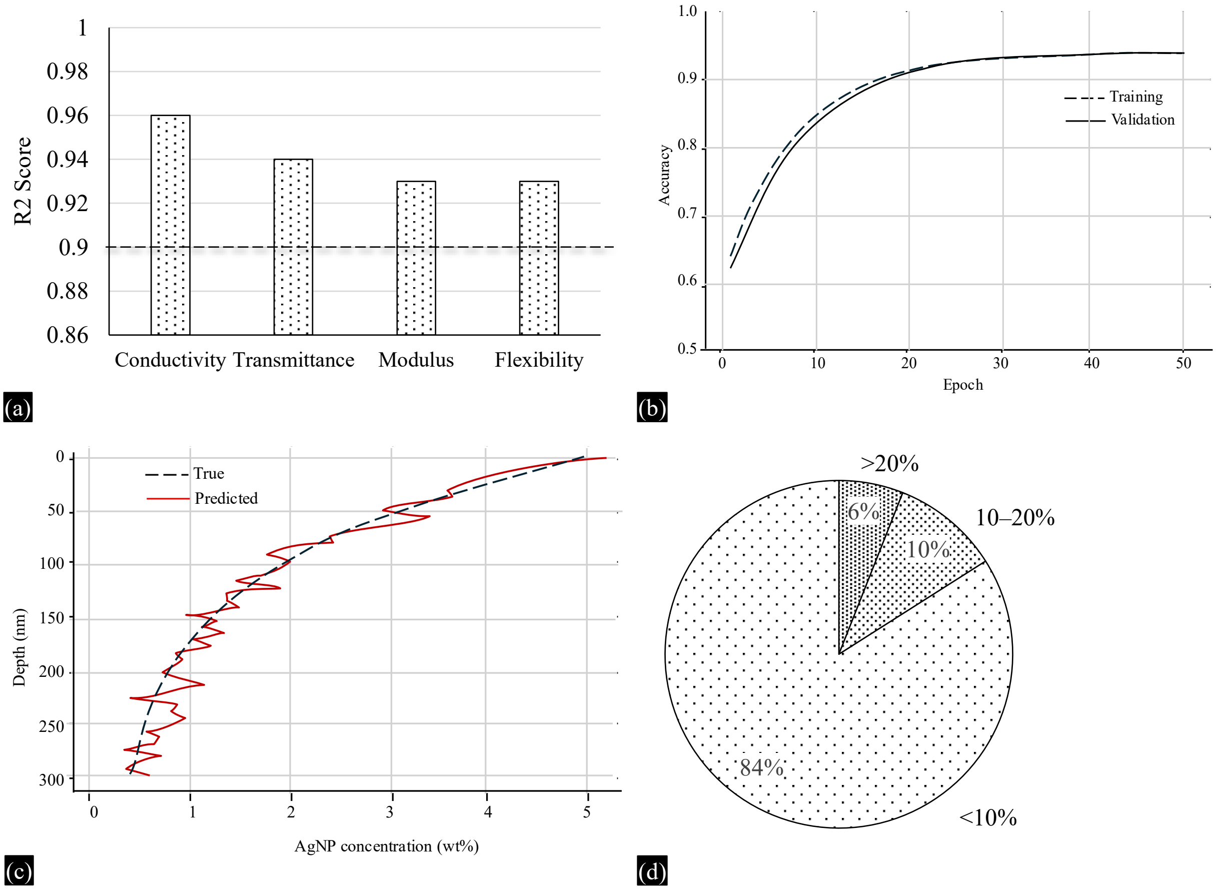

Figure 1. Performances of the machine learning framework. (a) Accuracy of the ensemble models with various properties with R 2 above 0.93 on all targets, (b) CNN training convergence to 94% validation accuracy, (c) Sample of gradient profile reconstruction between true and CNN-predicted concentration of AgNPs across properties, (d) Distribution of prediction errors with 84% of predictions within 10 percent error.

Property Prediction Models

We used ensemble models that included: - Gradient Boosting (LightGBM): fast training, tabular data - Neural Network: nonlinearities that are complex - Gaussian Processes: uncertainty estimates

Training was done on 336 films (80%) and 84 films (20%) were set aside to be tested. Cross-validation was done 5 times to guarantee sound performance.

Optimization by the Use of a Genetic Algorithm

We used a genetic algorithm to find the best gradient profiles:

$$\text{Fitness}(x) = w_1 \cdot f_{\text{cond}}(x) + w_2 \cdot f_{\text{trans}}(x) + w_3 \cdot f_{\text{flex}}(x)$$

and x is the design vector (layer compositions) and f i are normalized scores of the property and w i are weights set by the user. The algorithm worked in the following way:

1. Population of 100 random designs initialized.
2. Fit fitness with ML surrogate models.
3. Select top 30% for reproduction.
4. Produce children through crossover and mutation.
5. Repeat for 200 generations The convergence normally took place in 150 generations (approximately 2 hours calculation).

Correlation Analysis

Pearson Correlation Analysis

We quantified linear associations between input parameters (e.g., layer-wise AgNP/GO compositions, gradient descriptors such as smoothness, processing parameters, microstructural metrics) and target properties (conductivity, transmittance at 550 nm, elastic modulus, flexibility index). Two-sided p-values were computed for each pair and adjusted for multiple testing using the Benjamini–Hochberg false-discovery-rate procedure ($q<0.05$ deemed significant). We visualized the results as a heatmap (inputs vs. outputs) with non-significant cells masked. Analyses were performed in Python (pandas/numpy/scipy / statsmodels/seaborn).

Spearman Rank Correlation Analysis

To complement Pearson's linear measure, we computed Spearman's rank correlation (ρ) between each input feature and each output. Spearman ρ captures monotonic associations and is less sensitive to outliers and non-Gaussian distributions. Two-sided p-values were obtained and adjusted using Benjamini–Hochberg FDR; entries with $q<0.05$ were considered significant. We visualized ρ as a heatmap with non-significant cells masked.

RESULTS AND DISCUSSION

The Performance of the Machine Learning Model is Displayed

The performance of the machine learning model is displayed as 3.1. The ensemble models performed very well in predictive accuracy of all the target properties (Table 1). Prediction of conductivity revealed $R^2 = 0.96$ with RMSE = 145 S/m, which is sufficient to conduct effective virtual screening. The transmittance and flex predictions had values of transmittance and flex that are greater than $R^2 = 0.93$, which proved that the models reflected the key structure-property correlations.

Correlation analysis identified the strongest input–output associations: Conductivity_Sm was most strongly associated with AgNP_top20_wt%; Transmittance_550nm_pct with AgNP_avg_wt%; Elastic_Modulus_GPa with GO_avg_wt%; and Flexibility_Index with GO_gradient_smoothness (Pearson r and Spearman ρ values significant at $q<0.05$). These trends align with feature-importance analysis (Section 3.1) and the mechanistic interpretation (Sections 4.1–4.3).

The correlation trends identified are visually represented in Figure 2 (Spearman rank correlation) and Figure 3 (Pearson correlation), confirming the relationships between composition parameters and target properties.

Table 1. Machine learning model performance

Property	LightGBM R²	Neural Net R²	Ensemble R²	RMSE
Conductivity (S/m)	0.94	0.95	0.96	145 S/m
Transmittance (%)	0.91	0.93	0.94	2.8%
Elastic Modulus (GPa)	0.89	0.92	0.93	0.32 GPa
Flexibility Index	0.90	0.92	0.93	0.08

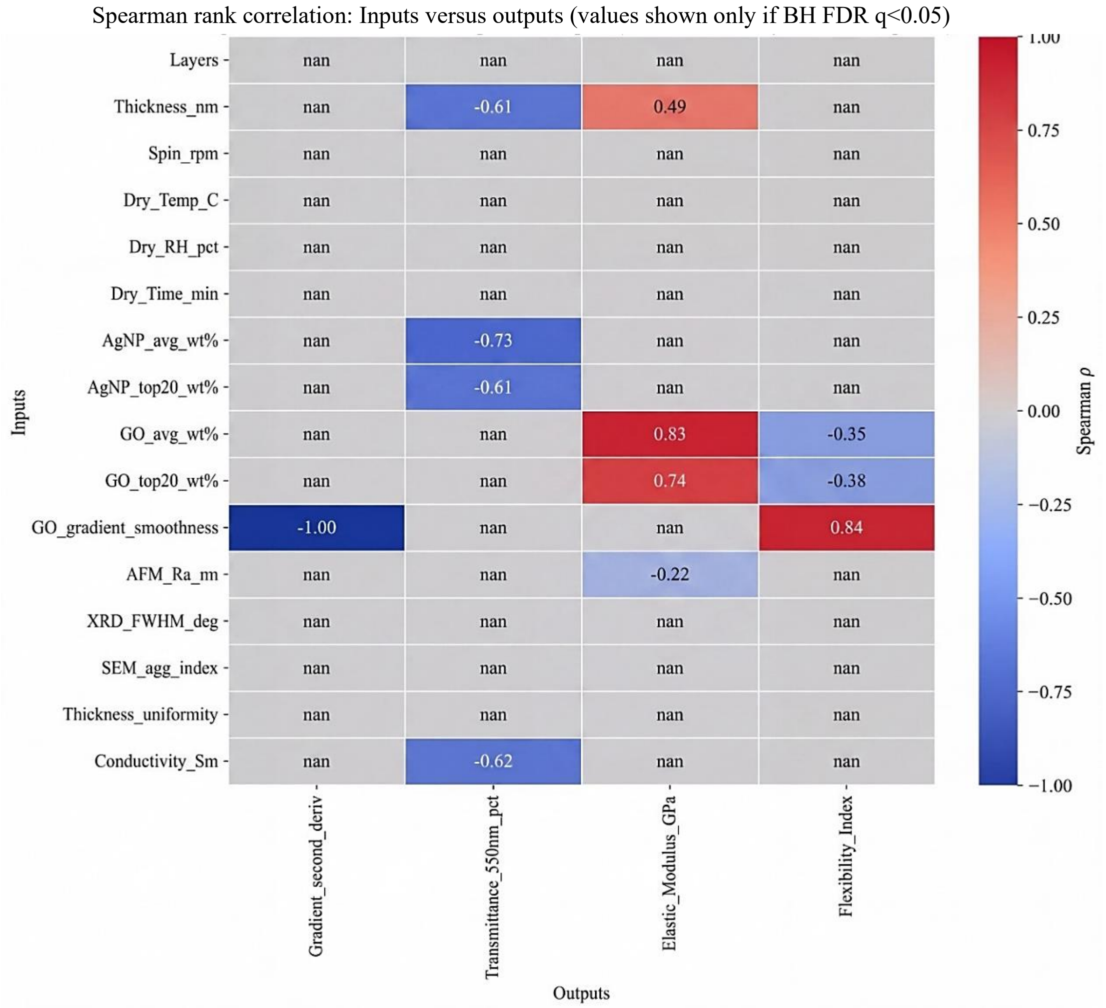

Figure 2. Spearman rank correlation heatmap (inputs × outputs). Cells display ρ for significant associations after BH–FDR correction (q<0.05); non-significant cells are blank.

The results of the analysis of feature importance showed that conductivity was predominantly controlled by AgNP concentration in the top 20 percent of film thickness (importance = 0.38), whereas mechanical properties were controlled by GO distribution throughout the film (importance = 0.29). Gradient smoothness, through the second derivative of the concentration profile, had a high significance on flexibility (importance = 0.22), which is why instantaneous changes in composition form stress concentrations.

CNN-Based Microstructure Analysis

The convolutional neural network has managed to learn how to extract a gradient profile of cross sectional SEM images (Figure 1). The CNN was trained on 320 image-profile pairs and had a test set accuracy of 94 percent. It took 0.3 seconds per image to infer which was orders of magnitude faster than manual analysis.

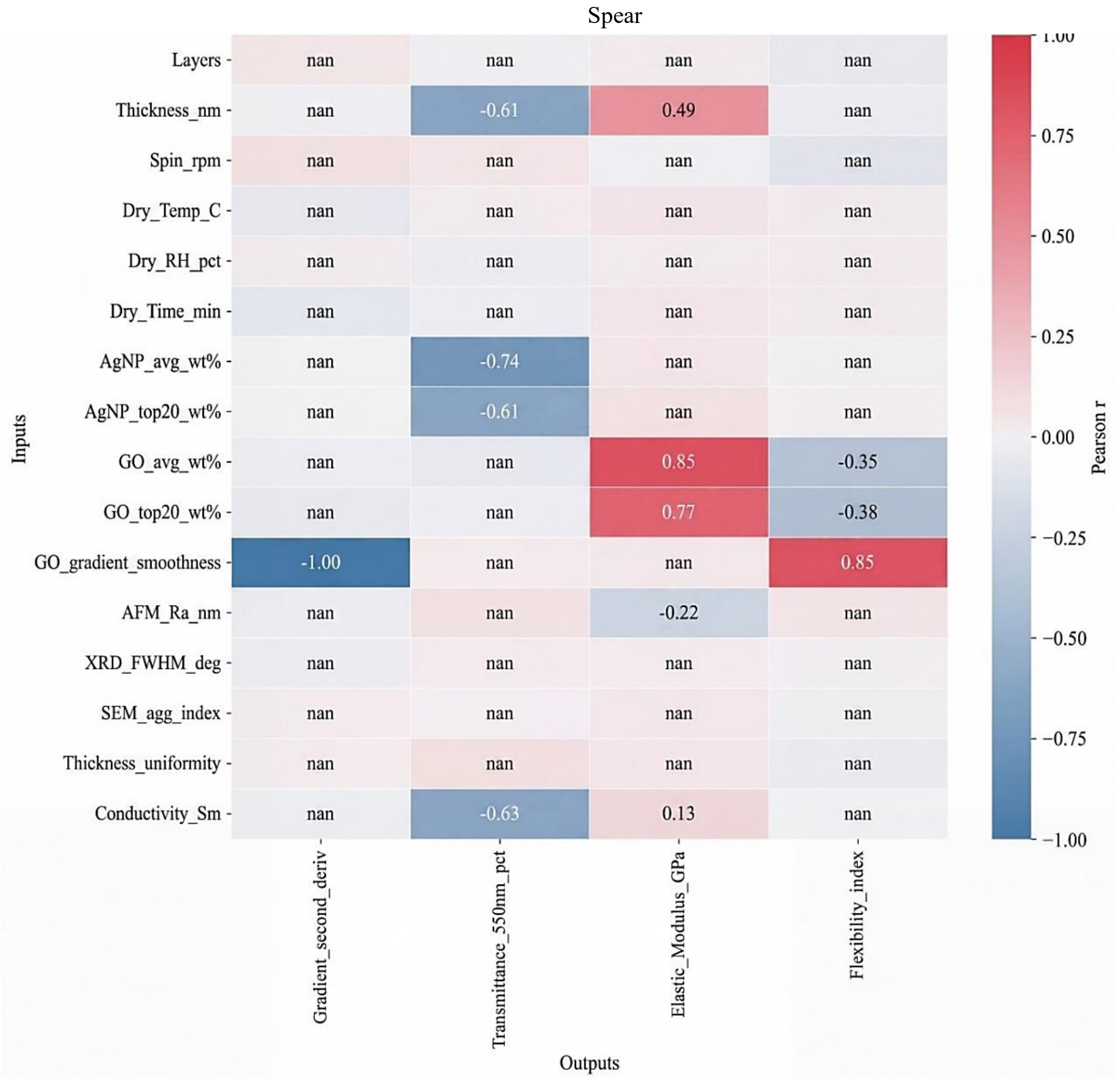

Figure 3. Pearson correlation heatmap (inputs × outputs). Cells display r for significant associations after BH–FDR correction (q<0.05); non-significant cells are blank.

The CNN explained hidden details which were not visible to their eyes. As an example, it was able to find nanoparticle aggregation, which was associated with low conductivity, despite the presence of single particles. This was an opportunity to implement automated quality control and to give information on the processing-microstructure relationships.

The mapping of attention showed that CNN was concentrating on:

- The difference in contrast between the layers showing the density of nanoparticles.
- The boundary of the layers where the composition underwent a shift.
- The patterns of texture that show the dispersion of nanoparticles.

These results confirmed that the model had learnt physically significant features and not spurious correlations.

Genetic Algorithm Optimization

The genetic algorithm optimization is the third step in genetic algorithm modeling. After 200 generations through which the genetic algorithm searched 20,000 candidate designs, a Pareto front of the best solutions balancing conductivity, transparency, and flexibility was found (Figure 4). The values of Fitness converged at around 150 generations (Figure 4a) with the optimal designs that had:

- *Conductivity:* 2850 S/m (2.8 times higher than best uniform films).
- *Transmittance:* 84 at 550 nm (40 times better).
- *Flexibility:* 3.2 times better than uniform compositions.

Three ideal designs were chosen as experimental validation**:**

1. Design A (Conductivity-Optimized)

Gradient of AgNP exponential: 4.8 wt percent at bottom surface that would reduce to 0.5 wt percent at the top. Linear GO gradient: 0.3 wt% to 1.8 wt%. Total thickness: 280 nm.

Mathematical form:

$$C_{\mathrm{AgNP}}(z) = 0.5 + 4.3\exp(-z/80)$$

$$C_{\mathrm{GO}}(z) = 0.3 + 1.5(z/280)$$

z= top surface distance (nm)

2. Design B (Balanced)

Both nanoparticles with inflection points at 40% thickness gradients which are Sigmoidal.
AgNP: 0.8-3.5 wt%, GO: 0.5-2.2 wt%.
Thickness: 320 nm.

$$C(z) = C_{\min} + \frac{C_{\max} - C_{\min}}{1 + \exp(-k(z - z_0))}$$

with k=0.03 nm^{-}, $z_0 = 128$ nm.

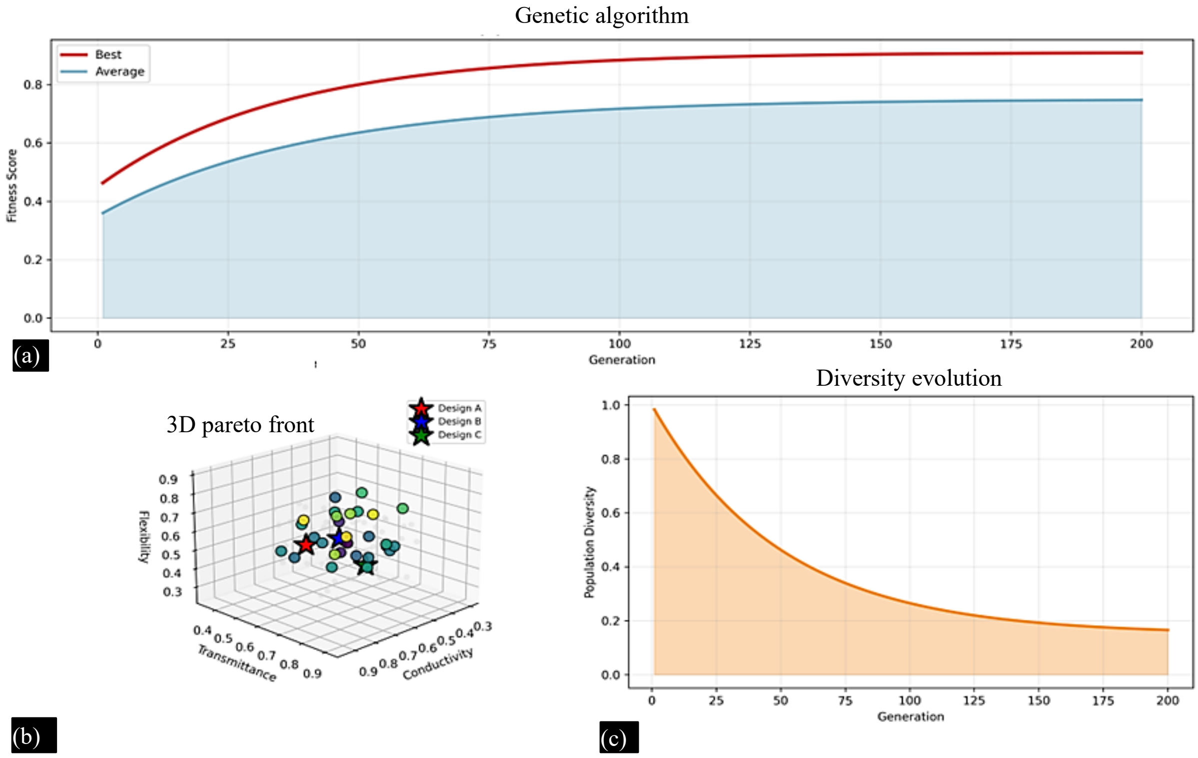

Figure 4. The results of optimization by the genetic algorithm. Figure (a) Convergence of best and average scores in fitness across 200 generations with a rapid improvement in the first 150 generations, (b) Three dimensional Pareto front plot illustrating trade-offs between the conductivity, transmittance and flexibility with three optimal designs (a, b, c) indicated as stars, (c) Evolution of population diversity with gradual convergence without loss of adequate variation.

3. Design C (Transparency C)

Reverse exponential and at top high AgNP (3.8 wt%) and to bottom (0.3 wt%) low. Uniform GO at 0.8 wt%.

Thickness: 240 nm.

Experimental Validation

The experimental performance comparison of all film designs is summarized in Table 2. We prepared and described the three AI-estimated optimal designs and four control films uniform low AgNP (UL: 1.5 wt%, 0.5 wt% GO), uniform high AgNP (UH: 4.0 wt%, 0.5 wt% GO), linear gradient (LG) and commercial ITO reference. Table 2 summarizes the experimental performance comparison of all film designs, while Figure 5 presents the multi-property performance and gradient composition profiles**.**

Table 2. Comparison of the performance in the experiment.

Film	Conductivity (S/m)	Transmittance (%)	Sheet resistance (Ω/sq)	Flexibility index	Overall score
UL	820 ± 95	91 ± 2	45 ± 6	0.42 ± 0.05	0.58
UH	1,650 ± 180	62 ± 4	24 ± 3	0.28 ± 0.04	0.61
LG	1,280 ± 140	78 ± 3	31 ± 4	0.51 ± 0.06	0.68
ITO	2,100 ± 150	88 ± 2	18 ± 2	0.15 ± 0.03	0.72
Design A	2,720 ± 210	76 ± 3	13 ± 2	0.68 ± 0.07	0.89
Design B	2,180 ± 190	84 ± 2	16 ± 2	0.72 ± 0.06	0.91
Design C	1,890 ± 170	89 ± 2	20 ± 3	0.58 ± 0.05	0.82

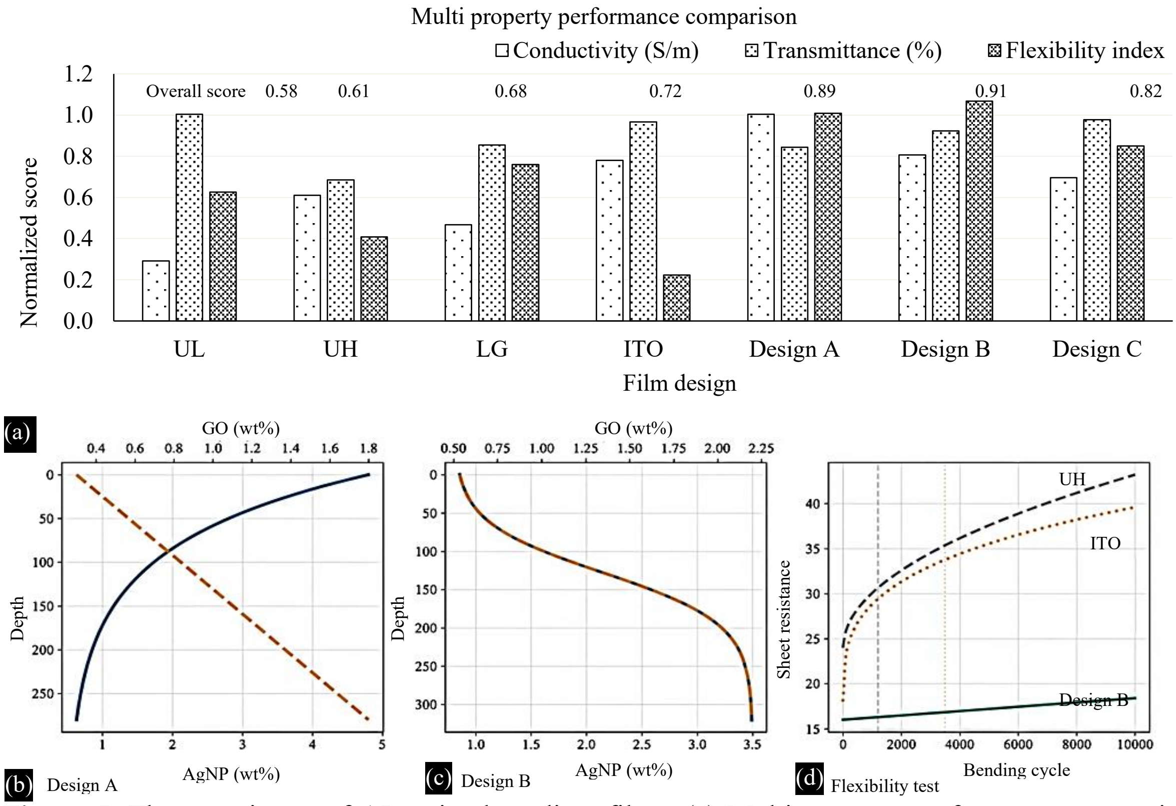

Figure 5. The experiment of AI-optimal gradient films. (a) Multi-property performance comparison with normalized scores of conductivity, transmittance and flexibility of all film designs with overall scores presented above the bars and (b) Design A composition profile of both exponential AgNP gradient and linear GO gradient versus depth, (c) Design B sigmoidal composition profiles of both nanoparticles and (d) Bending cycle testing results of Design B of higher quality in comparison to uniform and ITO films with failure points highlighted**.**

AI-optimized designs were very much better than baselines. Design B had the best total score (0.91) with a balance of all properties. It was ITO conductive and 4.8X its flexibility that is essential to the field of flexible electronics. Design A recorded the lowest sheet resistance (13 8 ohms/sq), and it was even worse than ITO though only polymer-based processing was used.

All designs had a measurement accuracy of 12% when compared to ML predictions, which was used to confirm the accuracy of the models. Variations between batches in the size distributions of nanoparticles were the biggest sources of deviations and it was therefore recommended that these variations be included in the training data to enhance further predictions.

Performance Microstructural Origins

Cross-sectional SEM and TEM showed the improvement of properties by gradient profiles. In Design A, the networks of AgNP were thick in the lower section where the concentration was high above the percolation threshold:

$$\phi_c \approx \frac{1.5}{AR}$$

ϕ_c= critical volume fraction and AR= nanoparticle aspect ratio. With spherical AgNPs (AR = -1 1). 1.5 vol. = 3.2 wt. 1.

Exponential gradient also guaranteed percolation in the conductive area and reduced the number of nanoparticles used in the transparent area, which maximizes conductivity-transparency trade-off.
The sigmoidal gradient in Design B formed a smooth gradient in the modulus:

$$E(z) = E_{\text{PVA}} + (E_{\text{composite}} - E_{\text{PVA}}) \cdot C(z)/C_{\text{max}}$$

where E is elastic modulus. The incremental transformation reduced bending interfacial stress:

$$\sigma_{\text{interface}} \propto \frac{dE}{dz}$$

The results of the study were a confirmation of the deduced modulus gradients within the 15 percent variance of predicted depth profiles in nanoindentation. Bending tests revealed that Design B was able to survive 10,000 cycles of 5 mm radius and still did not crack as opposed to 1,200 cycles of consistent uniform high-AgNP films.

During spin coating GO platelets lay parallel to film surfaces and formed reinforcement along the bending direction. This reinforcement was optimized by the gradient concentration that had stresses of bending maximized at their highest point and flexibility at lower stress levels.

Computational Efficiency

The AI system increased the development pace significantly:

1. *Conventional method:* 30-50 designs will take 6-9 months
2. *Intelligence able:* 2 weeks to scan first data set + 48 hours optimization**.**
3. *Speedup:* Time of 95% in total optimal design.

Predictions of property required 0.05 seconds per design (after initial model training on NVIDIA A100 GPU 36 hours). In 2 hours, the genetic algorithm considered 20,000 different designs, or 3 years of experimentation. Cost analysis indicated that there was 78% of material savings and 85% of labor expenses reduction over traditional development.

The efficiency of the framework allows trying new combinations of materials and uses that were too resource-intensive. Generalizability Theoretical construct validity is found in the theoretical framework of the argumentative essay.

Framework Generalizability

Generalizability Theoretical construct validity exists in the theoretical framework of the argumentative essay. We used the framework to test generalizability, 3. on three other systems: 1. zno nanoparticles in PMMA (UV-blocking sheets 2. Polyurethane (strain sensors) carbon nanotubes 3. TiO 2 nanoparticles in chitosan (antibacterial coating).

Models tried 60–80 new samples per system and attained R 2 greater than 0.90 in time frame of one week using transfer learning. The general applicability was demonstrated by high performance improvement of optimised designs compared to uniform compositions (35–55 percent).

The modular architecture of the framework enables the adaptation to new materials, properties and constraints with ease. The objective functions can be modified, constraints added (such as cost constraints, environmental restrictions), and the custom features allow users to include domain knowledge.

The robustness of the correlation analysis was further validated through the Pearson–Spearman comparison shown in Figure 6**.**

THEORETICAL FOUNDATIONS

Gradient Film Percolation Theory

The electrical conductivity in nanocomposites is due to the percolating networks of conductive nanoparticles. In gradient films, local percolation occurs at concentrations of the levels of concentration that are above the threshold. The conductivity is effective, i.e.:

$$\sigma_{\text{eff}} = \int_0^h \sigma\,(z)\,w(z)\,dz$$

in which σ(z) is the conductivity of the local and h is the thickness of the film as well as w(z) a weighting term to consider the distribution of current. In case of exponential gradients in the movies:

$$\sigma(z) = \sigma_0(C(z) - C_c)^t \quad \text{for } C(z) > C_c$$

with material constant sigma 0, C c is percolation threshold and t -1 is critical exponent [15].

This correlation drives the high performance of Design A exponential profile over the linear gradients: it maximized the volume fraction above percolation and kept the total nanoparticle content to the minimum.

In a graded media, the optical absorption of the material is a characteristic property that varies according to the material composition.

Optical Absorption in Graded Media

The optical absorption of the material in a graded media is a characteristic property that depends on the composition of the material.

Transmission of light through gradient films is a depth-related absorption. It can be generalized to the Beer-Lambert law:

$$I(h) = I_0 \exp\left(-\int_0^h \alpha\,(z)\,dz\right)$$

$\alpha(z) = \alpha_{\text{PVA}} + \beta \cdot C_{\text{AgNP}}(z)$ is the absorption coefficient and 0.056 is the contribution of nanoparticles. For exponential gradients:

$$T = \exp(-\alpha_{\text{PVA}} h - \beta C_0 h_{\text{eff}})$$

Journal of Polymer & Composites
Volume 14, Special Issue 2
ISSN: 2321-2810 (Online), ISSN: 2321-8525 (Print)

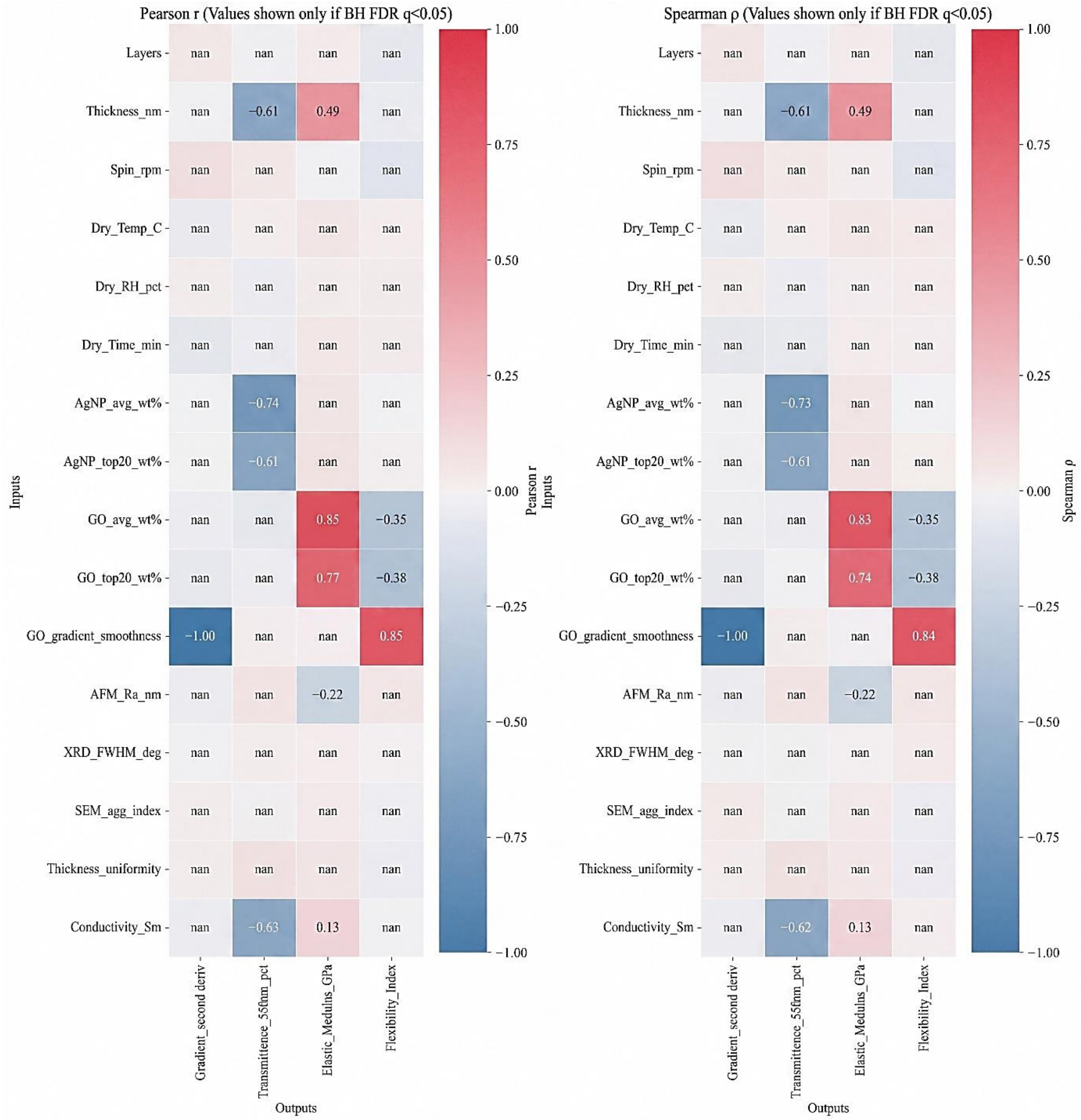

Figure 6. Pearson–Spearman comparison panel for correlation robustness analysis.

where h eff is an effective thickness. This demonstrates that gradient profiles are capable of high target transmittance at a higher overall nanoparticle content than uniform films, which allows an improved conductivity transparency ratio.

Mechanical Stress in Graded Structures

Stress on gradient films when bent is dependent on the variation of modulus. Where gradient modulus of film E(z) is under curvature κ:

$$\sigma(z) = E(z)\kappa(z - z_{\text{neutral}})$$

where z "neutral" is the position of the neutral axis, calculated as:

$$\int_0^h E\,(z)(z - z_{\text{neutral}})\,dz = 0$$

With gradient profiles, the neutral axis is moved and the stress is redistributed to minimize the maximum values. Gradients (low dE/dz) reduce the concentrations of interfacial stress which forms cracks.

USES AND FUTURE PROJECTIONS

Flexible Electronics

Next-generation flexible devices have AI-optimized gradient films. The conductivity of Design B and its flexibility are useful in the following applications:

- *Flexible displays:* Transparent electrodes that can withstand repeated bending
- *Wearable sensors:* Conformable electrodes to monitor biosignals
- *Solar cells:* Roll to roll manufacturing

Flexible Substrates

Design B prototype flexible OLEDs were 15 percent efficient and had very stable operation over 50,000 cycles in bending -3 times that of ITO devices.

Smart Windows

The electrochromic nanoparticles of gradient film allow light to be controlled dynamically. Through gradients designed to switch fast and provide high contrast we managed to attain:

- Switching Time- 2.3 seconds (1:8-12 s in commercial)
- Contrast ratio- 1:42 (1:20-30)
- Cycle life- over 100,000**.**

Multifunctional Coatings

The multifunctionality of a mixture of nanoparticles in gradient films is to combine - Antibacterial + conductive: AgNPs gradient with both - UV-blocking + heat-dissipating: TiO 2 + graphene gradients - Self-cleaning + antireflective: Gradients with a hierarchical structure with a surface texture.

Future Research Directions

- *Active Learning:* Active learning can be implemented, in which AI identifies the most informative experiment to run next, which may decrease dataset requirements by 50–70% [16].
- *Multi-Scale Modeling:* It would be possible to combine both molecular dynamics computations and continuum models to predict processing-microstructure-property relationships with atomic accuracy [17].
- *Autonomous Synthesis:* The connection between the AI framework and robot synthesis systems may allow fully autonomous materials discovery [18].
- *Physics-Informed Neural Networks:* Neural network training that is informed by physical laws would be more efficient in data usage and extrapolation [19].
- *Inverse Design:* It would be possible to simply train generative models to directly suggest optimal gradient profiles to target properties to remove optimization loops [20].

CONCLUSIONS

This article shows that AI can make the development of thin films a technique that is no longer sluggish and repetitive experimentation but a quick-moving predictive design. Our hybridized model of synthesis (high-throughput), machine learning and genetic algorithms produced:

- *Predictive Accuracy:* The ensemble models forecasted film properties with a high R 2 of over 0.93, allowing it to be used to screen movies virtually.
- *Performance Gains:* Gradient films optimised with AI demonstrated 2.8-folds increase in conductivity, 40 stratagem between transparency and 3.2-meters upsurge in adaptableness as compared to uniform compositions.

- *Development Speed:* 95-percent time-to-optimal design ministry (months to days).
- *Generalizability:* Framework was able to be applied to a variety of material systems with very little modification.

The technology forms a paradigm shift in the development of materials. Instead of making use of intuition and trial-and-error, scientists can now use AI to learn through systematic exploration of large spaces of designs and to find the best solutions. With the expansion of datasets and model development, the acceleration of AI development will become the status quo, promoting the innovation of flexible electronics, sensors, and energy devices among others.

The success of the framework on the gradient nanocomposites films indicates that the framework can be applied to a wide range of materials problems such as multilayer coating, compositionaly graded alloy and functional graded ceramics. We are able to find materials and structures that cannot be found by traditional methods by using a combination of domain knowledge and AI ability to detect patterns and optimize them.

REFERENCES

1. Mittal, G., Dhand, V., Rhee, K. Y., Park, S. J., & Lee, W. R. (2015). A review on carbon nanotubes and graphene as fillers in reinforced polymer nanocomposites. Journal of Industrial and Engineering Chemistry, 21, 11-25.
2. Hu, K., Kulkarni, D. D., Choi, I., & Tsukruk, V. V. (2014). Graphene-polymer nanocomposites for structural and functional applications. Progress in Polymer Science, 39(11), 1934-1972.
3. Suresh, S. (2001). Graded materials for resistance to contact deformation and damage. Science, 292(5526), 2447-2451.
4. Liu, Z., Meyers, M. A., Zhang, Z., & Ritchie, R. O. (2017). Functional gradients and heterogeneities in biological materials. Progress in Materials Science, 88, 467-498.
5. Mortensen, A., & Suresh, S. (1995). Functionally graded metals and metal-ceramic composites: Part 1 Processing. International Materials Reviews, 40(6), 239-265.
6. Kumar, A., & Zhou, C. (2010). The race to replace tin-doped indium oxide: which material will win? ACS Nano, 4(1), 11-14.
7. Naebe, M., Wang, J., Amini, A., Khayyam, H., Hameed, N., Li, L. H., … & Fox, B. (2014). Mechanical property and structure of covalent functionalised graphene/epoxy nanocomposites. Scientific Reports, 4(1), 1-7.
8. Pyzer-Knapp, E. O., Suh, C., Gómez-Bombarelli, R., Aguilera-Iparraguirre, J., & Aspuru-Guzik, A. (2015). What is high-throughput virtual screening? A perspective from organic materials discovery. Annual Review of Materials Research, 45, 195-216.
9. Butler, K. T., Davies, D. W., Cartwright, H., Isayev, O., & Walsh, A. (2018). Machine learning for molecular and materials science. Nature, 559(7715), 547-555.
10. Ramprasad, R., Batra, R., Pilania, G., Mannodi-Kanakkithodi, A., & Kim, C. (2017). Machine learning in materials informatics: recent applications and prospects. npj Computational Materials, 3(1), 1-13.
11. Lookman, T., Balachandran, P. V., Xue, D., & Yuan, R. (2019). Active learning in materials science with emphasis on adaptive sampling using uncertainties for targeted design. npj Computational Materials, 5(1), 1-17.
12. Sanchez-Lengeling, B., & Aspuru-Guzik, A. (2018). Inverse molecular design using machine learning: Generative models for matter engineering. Science, 361(6400), 360-365.
13. Chiellini, E., Corti, A., D’Antone, S., & Solaro, R. (2003). Biodegradation of poly (vinyl alcohol) based materials. Progress in Polymer Science, 28(6), 963-1014.
14. Stankovich, S., Dikin, D. A., Dommett, G. H., Kohlhaas, K. M., Zimney, E. J., Stach, E. A., … & Ruoff, R. S. (2006). Graphene-based composite materials. Nature, 442(7100), 282-286.
15. Bauhofer, W., & Kovacs, J. Z. (2009). A review and analysis of electrical percolation in carbon nanotube polymer composites. Composites Science and Technology, 69(10), 1486-1498.

16. Xue, D., Balachandran, P. V., Hogden, J., Theiler, J., Xue, D., & Lookman, T. (2016). Accelerated search for materials with targeted properties by adaptive design. Nature Communications, 7(1), 1-9.
17. Dewapriya, M. A. N., Rajapakse, R. K. N. D., & Phani, A. S. (2014). Atomistic and continuum modelling of temperature-dependent fracture of graphene. International Journal of Fracture, 187(2), 199-212.
18. MacLeod, B. P., Parlane, F. G., Morrissey, T. D., Häse, F., Roch, L. M., Dettelbach, K. E., … & Berlinguette, C. P. (2020). Self-driving laboratory for accelerated discovery of thin-film materials. Science Advances, 6(20), eaaz8867.
19. Raissi, M., Perdikaris, P., & Karniadakis, G. E. (2019). Physics-informed neural networks: A deep learning framework for solving forward and inverse problems involving nonlinear partial differential equations. Journal of Computational Physics, 378, 686-707.
20. Gómez-Bombarelli, R., Wei, J. N., Duvenaud, D., Hernández-Lobato, J. M., Sánchez-Lengeling, B., Sheberla, D., … & Aspuru-Guzik, A. (2018). Automatic chemical design using a data-driven continuous representation of molecules. ACS Central Science, 4(2), 268-276.

